Supplementary Figures

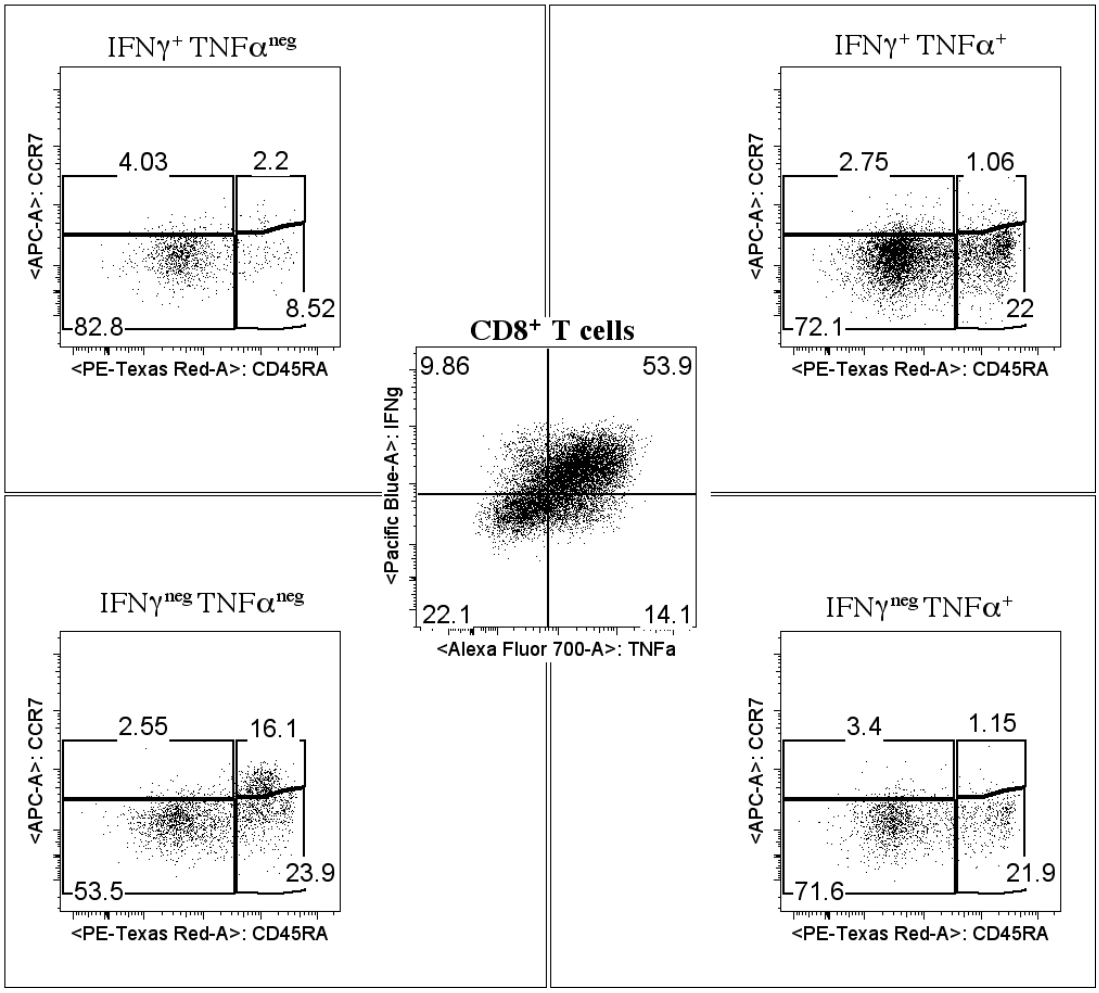

Figure S1: IFNγ and TNFα are produced only by memory CD8$^+$ T cells. Dot plots present cytokine produced by HD CD8$^+$ T cell subsets after P/I stimulation on WB. The staining panel used in this analysis was modified from the original panel described in Table 3A by replacing mouse anti-human IL-21 Al647 by the mouse anti-human CCR7 APC (R&D clone 150503) allowing to discriminate Naive (CD45RA$^+$CCR7$^+$, upper right panel), TEMRA (CD45RA$^+$CCR7^{neg}, upper left panel), Effector Memory (CD45RA^{neg}CCR7^{neg}, lower left panel) and Central Memory (CD45RA^{neg}CCR7$^+$, lower right panel) CD8+ T cell subsets producing IFNγ/TNFα. The majority of TNFα/IFNγ production is detected within CCR7^{neg}CD8$^+$ effector T cells.

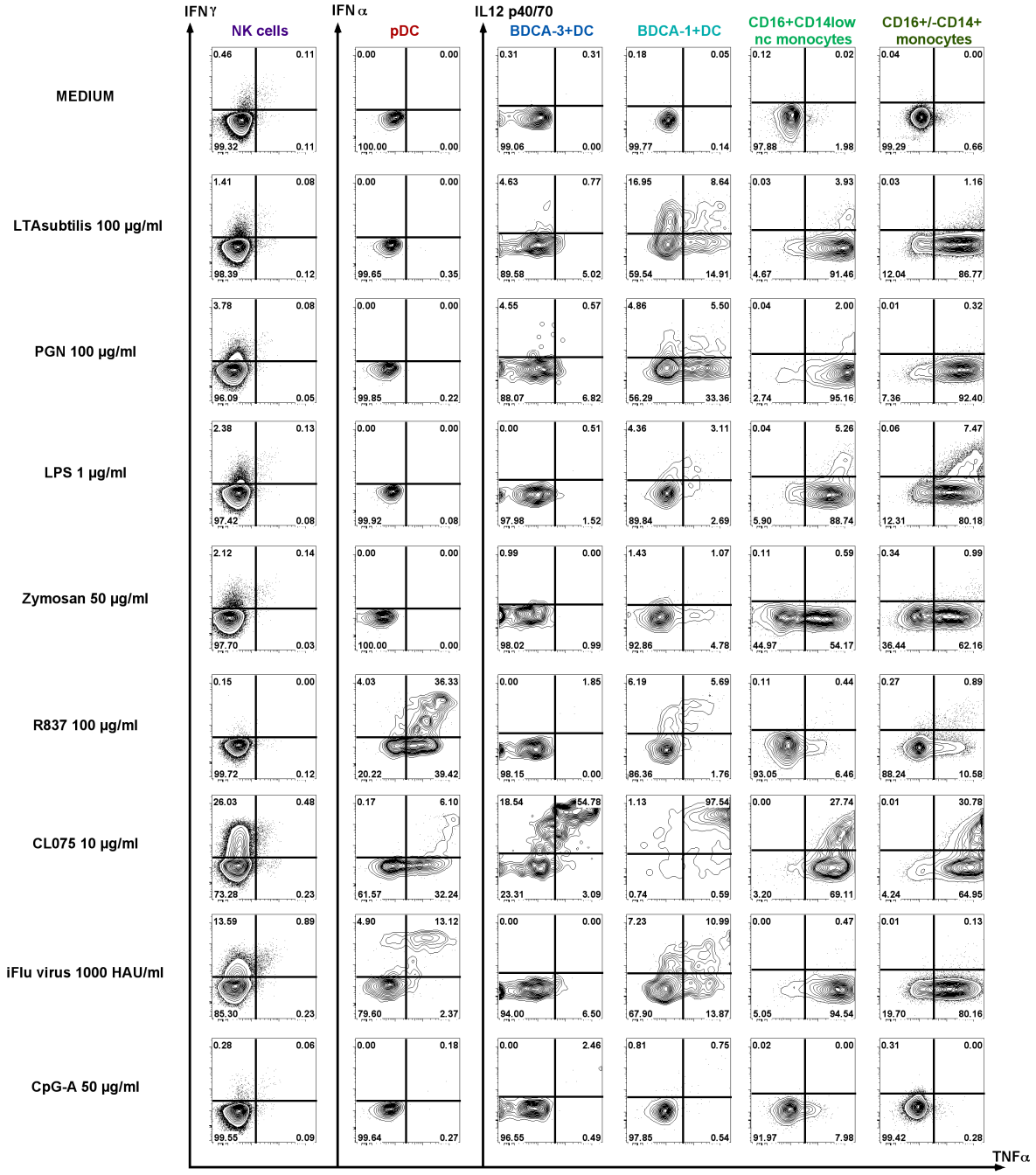

Figure S2: Capacity of innate immune cell subsets to produce cytokines in response to other signals. WB was incubated for 5 hours in presence of activators listed in **Table 2**. Brefeldin A was added after 1 hour and cells were then collected at 5h, and after red blood cell lysis membrane staining was performed to define the different subsets and after fixation and permeabilization, intracytoplasmic staining was performed to detect cytokine production. Dot plots present cytokine intracytoplasmic staining's to evaluate production of IFNγ/TNFα by NK cells or IFNα/TNFα by pDC as well as IL-12p40/TNFα by mDC (BDCA-3^{+}, BDCA-1^{+}) or monocyte (CD14^{+}CD16$^{+/-}$, CD14^{low}CD16^{+}) subsets according to the activator tested.

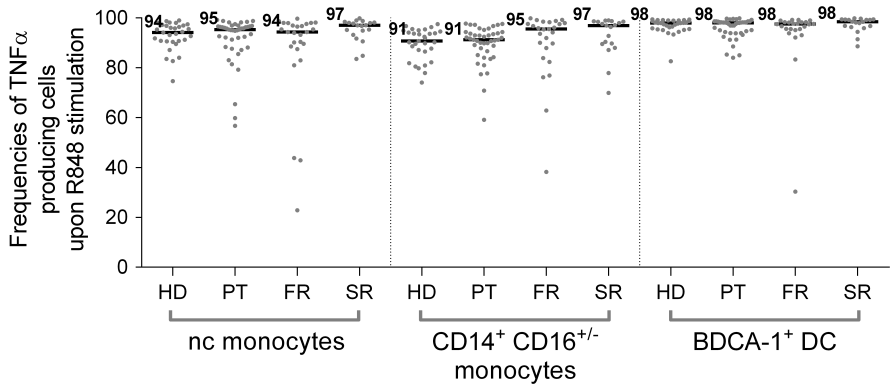

Figure S3: TNFα production by monocytes subsets and BDCA-1$^+$ DC was not altered in periphery during breast tumor progression after R848 activation.

The capacity of monocytes ($CD14^+CD16^{+/-}$, $CD14^{low}CD16^+$) subsets and BDCA-1^+ DC to produce TNFα after TLR7/8 ligand (R848, 10 μg/ml) stimulation was assessed on WB on BC patients' cohorts at different stages (PT (n=46), FR (n=34), SR (n=20)) and compared to a HD cohort (=31) and presented as percentage of cell subset producing TNFα in the different cohorts.

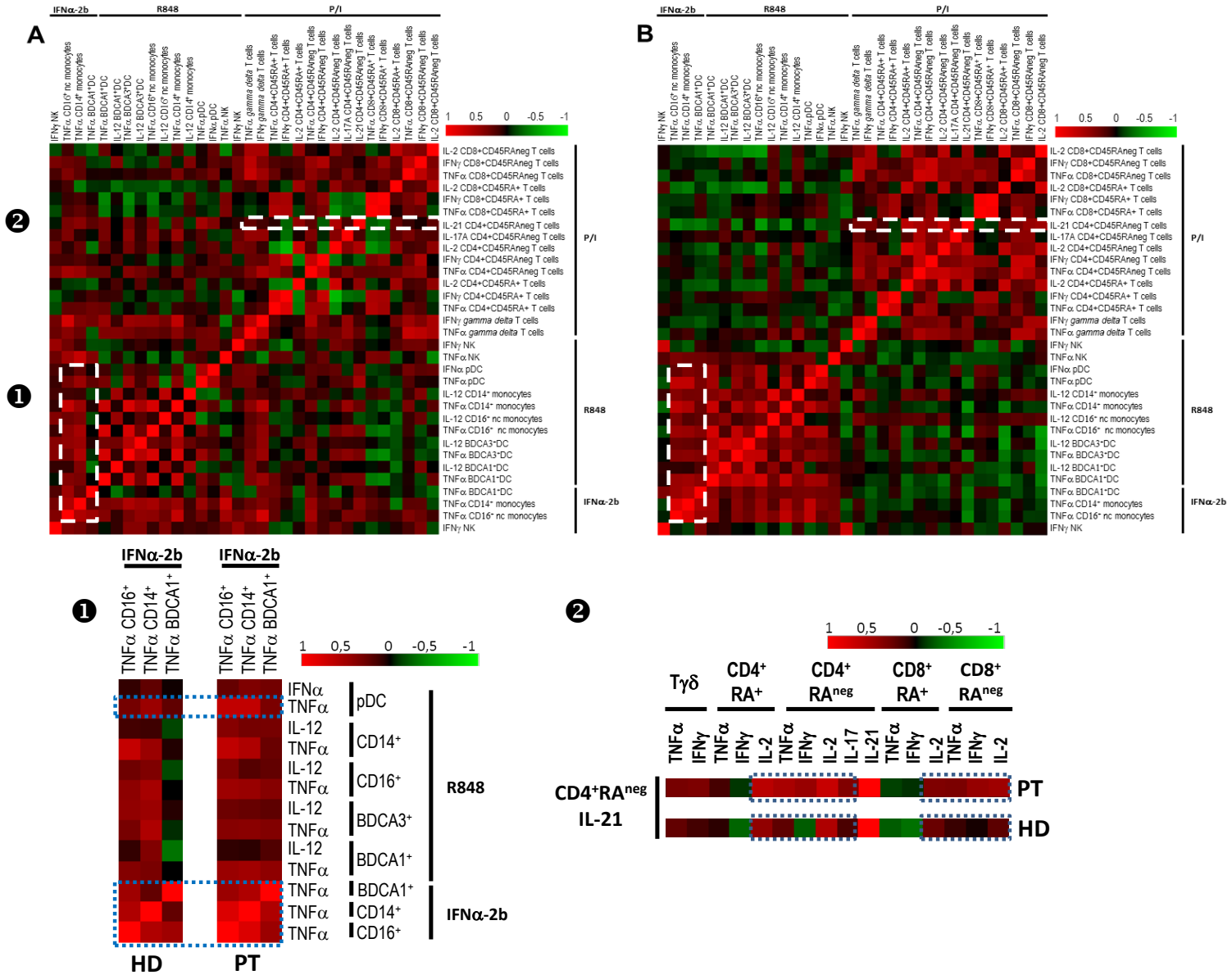

Figure S4: No correlation between innate and adaptive immune alterations within the PT cohort Heat maps representation of the Spearman correlations between cytokines (IL-12p40, TNFα, IFNγ, IFNα) produced by the different innate immune cell subsets (IFN-α2b, R848) and cytokines (IL-2, IL-17A, IL-21, IFNγ, TNFα) produced by the adaptive immune cell subsets after P/I stimulation on HD (A) and PT (B) cohorts. A focus on innate immune alterations (①) was extracted from both HD and PT panels and compared. A focus on correlations associated with IL-21 produced by CD45RA^{neg} CD4^{+} T cells (②) was extracted from both HD and PT panels and compared.

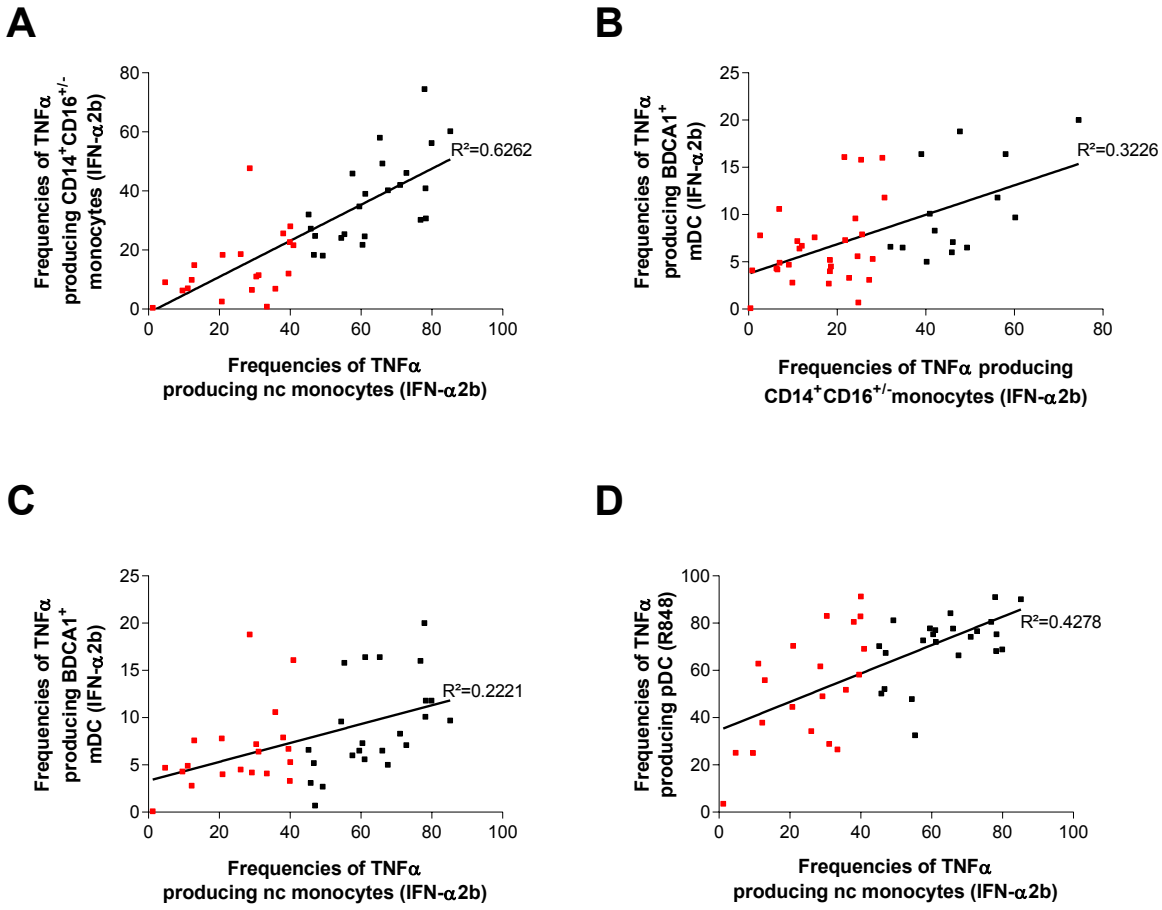

Figure S5: Coordinated alteration of TNFα production by innate immune cells under IFN-α2b and R848 activation in PT cohort. A-C Pairwise representation of percentage of cells ($CD14^+$ monocytes, $CD16^+$ nc-monocytes, $BDCA1^+$ DC) producing TNFα after IFNα-2b stimulation. D- Pairwise TNFα production by IFN-α2b-stimulated $CD16^+$ nc-monocyte and R848-stimulated pDC.

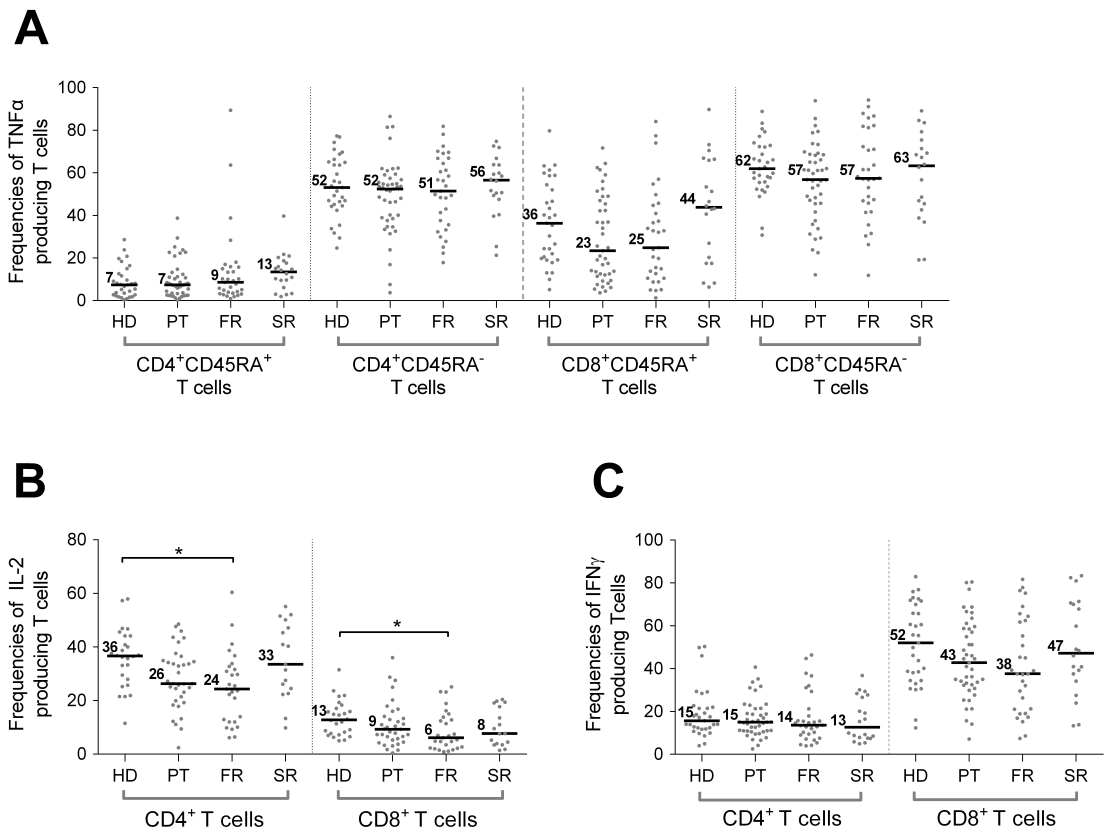

Figure S6: T cell subsets functional alterations observed in periphery during breast tumor progression. The functionality of T cell subsets was assessed on WB after short term polyclonal stimulation (P/I) in presence of brefeldin A on BC patients' cohorts at different stages (PT (n=46), FR (n=34), SR (n=20)) and compared to a HD cohort (=31) and presented as percentage of cell subset producing a specified cytokine in the different cohorts: percentage of TNFα production (A) by $CD4^+$ and $CD8^+$ T cell subsets ($CD45RA^+$ and $CD45RA^{neg}$), percentage of IL-2 (B) and IFNγ (C) production by $CD4^+$ and $CD8^+$ T cells. *: p-value < 0.05.

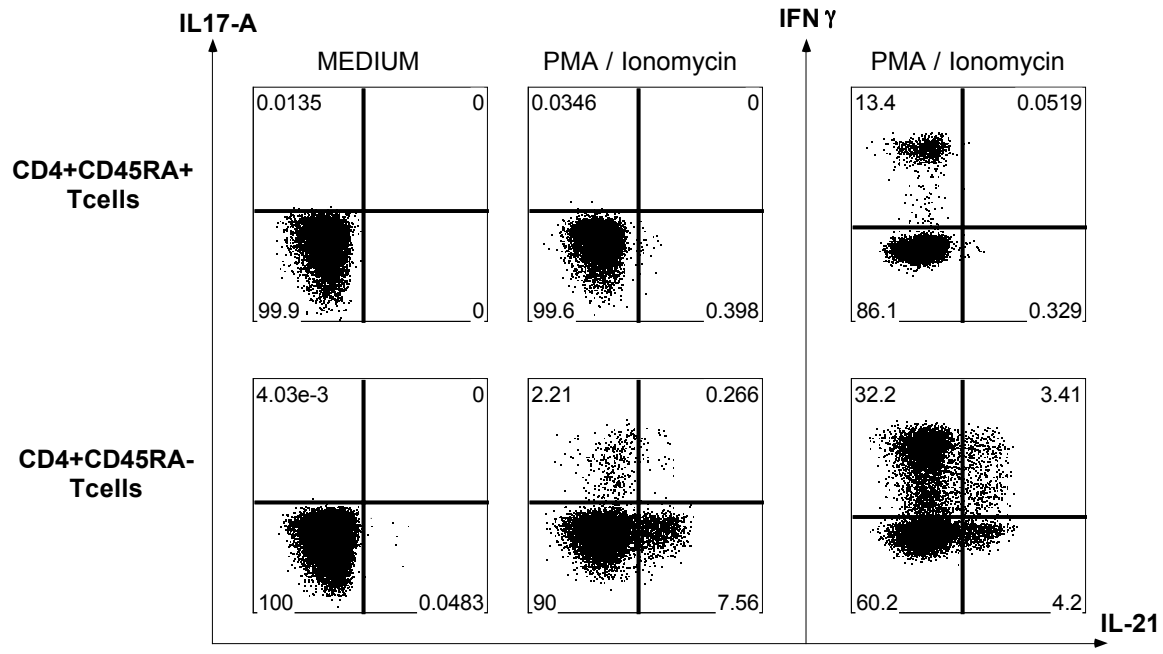

Figure S7: IL-17 and IL-21 production by CD4+ T cells – Validation of the specificity of the staining. Intracytoplasmic detection of IL-17 and IL-21 were performed on $CD4^+$ T cell subsets ($CD45RA^+$ and $CD45RA^{neg}$) after 5 hours incubation without activator (resting) or PMA/ iomomycin (P/I). The specificity of IL-21 staining was demonstrated by the lack of $IL\text{-}21^+$ cells detection i) in resting condition in both cell subsets and ii) in the P/I-activated $CD45RA^+$ $CD4^+$ cell subset.

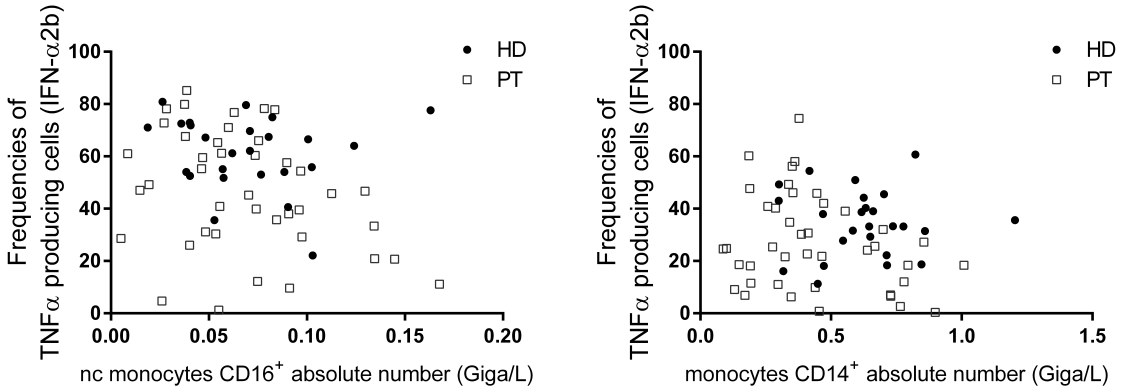

Figure S8: Absence of correlation between the monocyte subpopulations absolute number and their functional alterations. Correlations between frequencies (%) of TNFα producing cells and their absolute number (Giga/L) in PT (o) and HD (●) cohorts for $CD16^+$ nc-monocytes (A) or $CD14^+$ monocytes (B) subpopulations**.**